ORGANOMETALLICS

Article

Cite This: *Organometallics* XXXX, XXX, XXX−XXX

Catalytic-Site-Mediated Chain-End Control in the Polymerization of *rac*-Lactide with Copper Iminopyrrolide Complexes

Pargol Daneshmand, José L. Jiménez-Santiago, Maxime Aragon--Alberti, and Frank Schaper*

Centre in Green Chemistry and Catalysis, Department of Chemistry, Université de Montréal, C. P. 6128 Succ. Centre-Ville, Montréal, Quebec H3T 3J7, Canada

Supporting Information

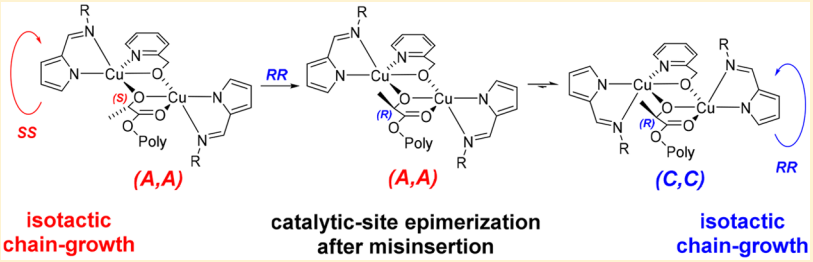

ABSTRACT: Reaction of copper(II) methoxide with *N*-R-2-iminopyrroles (LH) and pyridylmethanol (R′OH) provided the dinuclear complexes $\{LCu(\mu\text{-}OR')\}_2$ (R = naphtyl, $CHPh_2$, 2,6-xylyl, 2,6-diisopropylphenyl (diip), or *p*-bromobenzyl). All complexes crystallized as dinuclear compounds with a square-pyramidal coordination geometry around copper and either imine or pyridine (for R = diip) in the apical position. The naphthyl-substituted complex was inactive in *rac*-lactide polymerization at room temperature in benzene. All other complexes showed good activity with apparent rate constants of k_{obs} = 0.16(1)−1.89(8) h^{-1} at 2 mM catalyst concentration. All complexes showed a preference for slight isotactic monomer enchainment with P_m = 0.60−0.68. Stereoerror analysis indicate that the chain-end determines stereocontrol. A dependance of stereocontrol on the steric bulk of the ligand, on the initial monomer concentration and on the symmetry of the catalytic site support that the chiral information on the chain-end is mediated via the catalytic site (catalytic-site-mediated chain-end control).

INTRODUCTION

Polylactic acid (PLA) is the most important biodegradable polyester and typically obtained by ring-opening polymerization of lactide, the dimeric anhydride of lactic acid (Scheme 1).[1−11] Given its increasing economic importance and the currently unselective polymerization catalysis employed by industry, a large number of academic studies have focused with varying success on providing catalyst systems which allow the control of stereochemistry and reactivity in lactide polymerization.[12−38] Unlike the industrially employed polymerization of *L*-lactide, which can only provide isotactic PLLA, polymerization of racemic lactide can give rise to atactic polymer in the absence of stereocontrol. Stereocontrolled polymerization provides isotactic or heterotactic polymer with different degrees of stereoselectivity (Scheme 1), of which only isotactic PLA is of current industrial interest. Typically, high degrees of heterotacticity are comparatively easily achieved, while highly active, isoselective polymerization still poses a catalytic challenge.[39−48] Coordination−insertion polymerization catalyzed by a discrete metal alkoxide species is the most employed mechanism.

Scheme 1

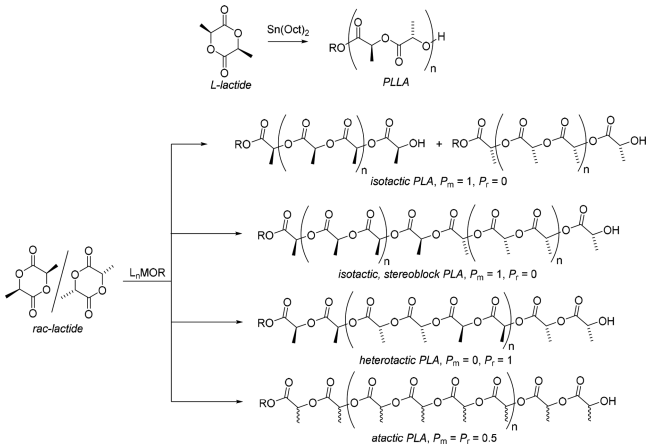

For various reasons, such as the general biocompatibility and the ease of complex characterization by ^{1}H NMR, most studies focused on d^0- or d^{10}-metal systems. Mid- to late d^n-transition metal complexes, on the other hand, have been sparingly studied. Very few studies investigated the performance of Cr,[49] Mn,[50−53] or Co systems.[51,54,55] Next to iron,[52,56−81] copper complexes received the highest attention.[82−104] We have reported that copper diiminopyrrolide complex **1** polymerizes *rac*-lactide with an isoselectivity of P_m = 0.7 at room

Received: April 3, 2018

DOI: 10.1021/acs.organomet.8b00196
Organometallics XXXX, XXX, XXX−XXX

temperature (Scheme 2).[94] Isoselective stereocontrol was unprecedented for copper complexes. The copper complexes

Scheme 2

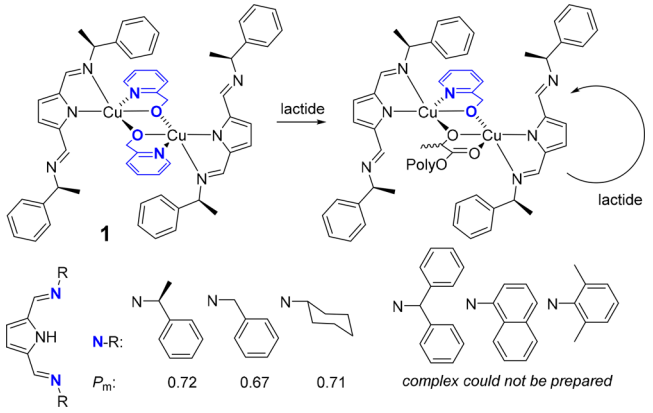

remain dinuclear throughout polymerization and successful stereocontrol depends on the presence of a bridging pyridylmethoxide ligand in the active species (Scheme 2).[85]

The stereocontrol mechanism proposed for lactide polymerization with copper iminopyrrolide complexes was catalytic-site-mediated chain-end control.[105,106] In this mechanism the chiral information is derived from the polymer chain end, which in turn determines the configuration of the flexible catalytic site. Monomer selectivity is then either enhanced or even determined by the configuration of the catalytic site. The mechanism is based on initial observations by Carpentier and Okuda that increased flexibility of the ligand/catalytic site led to increased heterotactic stereocontrol (Scheme 3).[105,106] Okuda proposed that heterotactic stereocontrol involves catalytic-site inversion after each insertion step.[105] Davidson proposed that a similar mechanism is in place for C_3-symmetric germanium and zirconium complexes.[107,108] Jones obtained isotactic PLA using zirconium complexes with either chiral or achiral ligands.[109,110] With chiral ligands, the complexes are locked into either Δ- or Λ- configuration and stereocontrol follows catalytic-site control. Achiral ligands allow Δ/Λ-isomerization, and epimerization of the catalytic site after a misinsertion led to stereoblock PLA obtained by (catalytic-site-mediated) chain-end control. Copper diiminopyrrolides, such as **1**, follow a similar mechanism, in which catalytic-site epimerization is assisted by coordination of the pendant imine (Scheme 4). A catalytic-site-

Scheme 4

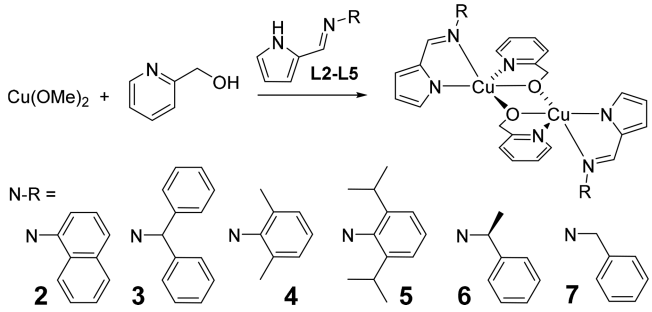

mediated chain-end control combines advantages of the more typical catalytic-site control and chain-end control mechanisms: (a) Chain-end control and catalytic-site control are often both present in lactide polymerization and in isotactic catalysts often with opposing stereoselectivities. (b) Chain-end control provides longer isotactic blocks with the same degree of control, since only one *r*-dyad is introduced per stereoerror. (c) Chain-end control mechanisms are less influenced by fast chain-transfer reactions and thus more suitable for immortal polymerizations. (d) Since monomer selection is governed by the catalytic-site, stereocontrol can thus be more directly influenced than in pure chain-end control. (e) No chiral ligands are required as long as a chiral catalytic site is formed. Despite the advantages of this mechanism, only the very few cases above have been reported, and the stereocontrol mechanism was often more postulated than proven. The same, unfortunately, was also true for diiminopyrrolide complex **1**. In the following we will offer further evidence to confirm the existence of this rather unusual stereocontrol mechanism.

RESULTS AND DISCUSSION

Impact of Sterically Bulky Ligands on Stereocontrol. Given the strong implication of the catalytic site in the

Scheme 3. Catalyst Systems Showing Catalytic-Site-Mediated Chain-End Control[a]

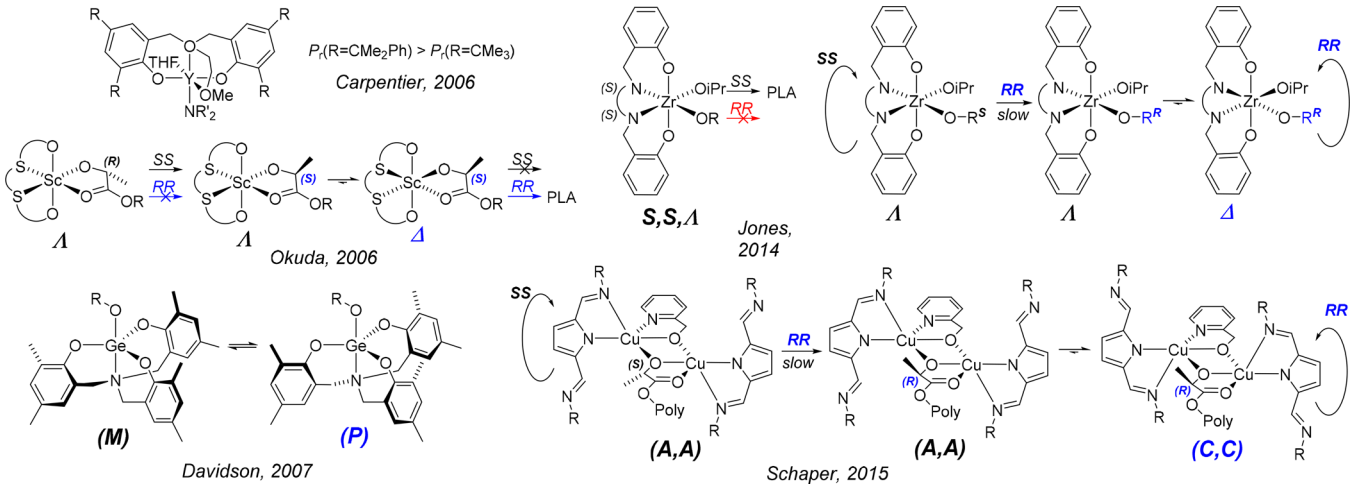

[a]*RR* and *SS* denote *R,R*- and *S,S*-lactide.

DOI: 10.1021/acs.organomet.8b00196
Organometallics XXXX, XXX, XXX−XXX

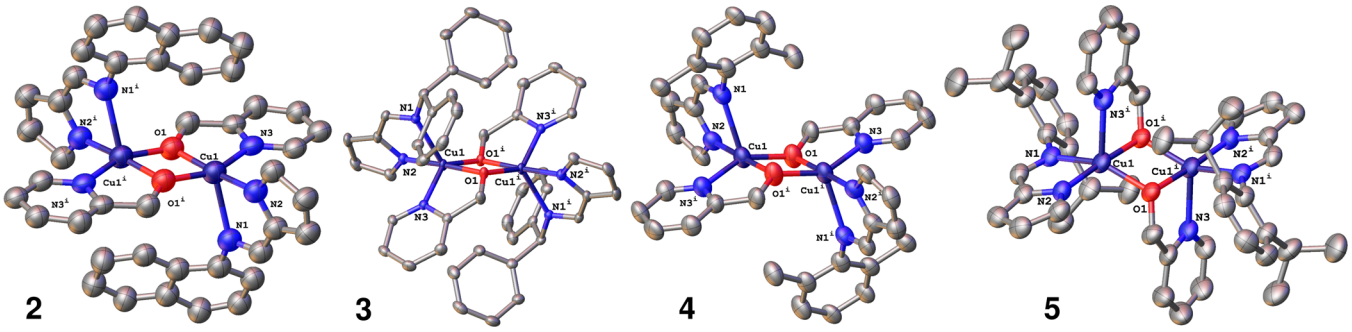

Figure 1. Crystal structures of **2**–**5**. Thermal ellipsoids are drawn at 50% probability (at 30% for **2**). Hydrogen atoms, a second independent molecule (**4**), and the minor component of *N*-aryl disorder (**4**) omitted for clarity.

Table 1. Bond Distances [Å] and Bond Angles [deg] in Iminopyrrolide Copper Complexes

	2	3	4[a]	5	9	6[a,b]	7[c]
Cu–$N_{pyrrole}$	1.98(2)	1.936(2)	1.938(7),1.930(8)	1.952(4)	1.934(8)	1.931(1), 1.935(1)	1.960(2)
Cu–N_{imine}	2.37(2)	2.314(2)	2.421(7), 2.374(8)	2.076(4)	2.295(8)	2.317(2), 2.398(1)	2.047(2)
Cu–$N_{pyridine}$	1.953(19)	2.049(2)	2.011(8), 2.000(8)	2.202(4)	2.034(8)	2.022(1), 2.026(1)	2.173(2)
Cu–O_{short}	1.942(16)	1.931(1)	1.929(6), 1.925(7)	1.962(3)	1.937(6)	1.927(1), 1.931(1)	1.974(2)
Cu–O_{long}	1.976(15)	1.974(1)	1.942(6), 1.953(6)	1.965(3)	1.967(6)	1.951(1), 1.951(1)	1.986(2)
Cu–Cu	3.030(7)	3.018(1)	3.025(3), 2.996(3)	3.0098(12)	3.025(3)	3.0, 3.1	2.992(1)
C6–N_{imine}–Cu	139.6(17)	136.4(1)	139, 138[d]	128.2(3)	134[d]	137.2(1), 134.8(1)	128.9(2)
τ	0.3	0.7	0.5, 0.5	0.4	0.5	0.4, 0.4	0.6, 0.6
group in apical position	imine	imine	imine, imine	pyridine	imine	imine	pyridine

[a]Two independent molecules in the asymmetric unit. [b]Taken from ref 85. [c]Taken from ref 84. [d]Averaged value of the observed disorder.

Table 2. *rac*-Lactide Polymerizations with 2–5 and 9[a]

catalyst	final conversion (time)	k_{obs} [h^{-1}]	M_n[b]	M_n (calcd)[c]	M_w/M_n	# chains[d]	P_m[e]
2	4–8% (24–32 h)[f]						
3	83% (27 h)	0.16(1)	12.2 kDa	12.0 kDa	1.6	1.0	0.57
4	99% (21 h)	1.89(8)	8.3 kDa	14.3 kDa	1.7	1.7	0.68
5	99% (3 h)	1.74(8)	15.9 kDa	14.3 kDa	1.8	0.9	0.65
5 + 1 Ph_3COH	95% (2 h)	1.79(3)	10.4 kDa	13.7 kDa	1.3	1.3	0.65
6[g]	99% (24 h)	1.29(1)	16.9 kDa	14.3 kDa	2.2	0.8	0.63
7[h]	99% (32 h)	1.07(4)	7.0 kDa	14.3 kDa	2.1	2.1	0.60
9	99% (23 h)	0.55(1)	11.1 kDa	14.3 kDa	1.6	1.3	0.60

[a]Conditions: C_6D_6, RT, [lactide] = 200 mM, $[L_2Cu_2(OR)_2]$ = 2 mM. The time of final conversion should not be considered a measure of activity but indicates after what time the reaction was quenched. [b]M_n and M_w determined by size exclusion chromatography vs polystyrene standards, with a Mark–Houwink correction factor of 0.58. [c]M_n expected if one alkoxide per catalyst dimer initiates polymerization, calculated from [lactide]/[cat]·conversion·$M_{lactide}$ + M_{ROH} [d]Number of chains per catalyst dimer, calculated from the ratio of expected and obtained polymer molecular weight. [e]P_m determined from decoupled ^{1}H NMR by $P_m = 1 - 2 \cdot I_1/(I_1 + I_2)$, with I_1 = 5.20–5.25 ppm (*rmr*, *mmr*/*rmm*), I_2 = 5.13–5.20 ppm (*mmr*/*rmm*, *mmm*, *mrm*). [f]Two experiments. [g]Taken from ref 85. [h]Taken from ref 84.

proposed stereocontrol mechanism, a notable influence of the steric bulk provided by the ligand on selectivity would have been expected. Unfortunately, variations of the *N*-substituent in **1** either provided complexes with very similar stereocontrol or, for sterically demanding *N*-$CHPh_2$, *N*-naphthyl, or *N*-xylyl substituents, the complexes were synthetically not accessible (Scheme 2).[84] Influence of ligand steric bulk was thus investigated for the respective *mono*iminopyrrolide complexes, in the expectation that the removal of one imino-substituent would allow the incorporation of a wider range of *N*-substituents.

Synthesis of ligands **L2**–**L5** followed either literature protocols or procedures successfully employed for similar ligands (see the Experimental Section). Corresponding monoiminopyrrolide complexes **2**–**4** were accessible using the same synthetic protocols employed for **1** (Scheme 4). In addition, complex **5**, containing a *N*-2,6-diisopropyphenyl (diip) substituent was prepared using the same methodology. Monoiminopyrrolide complexes **6** and **7** with methylbenzyl and benzyl *N*-iminosubstituents have been prepared previously.[85,94]

All complexes were characterized by X-ray diffraction studies. Previously obtained diimino- and monoiminopyrrolide complexes LCu(OR) typically form dinuclear copper complexes with a square-pyramidal coordination geometry around copper. The pyrrolide nitrogen and the bridging alkoxides were always found in the equatorial plane, while either the pyridyl or the imino group occupied the axial position.[84,85,94] Complexes **2**–**5** follow the same structural pattern (Figure 1): Despite τ values up to 0.7,[111] the coordination geometry around copper is best described as square-pyramidal with two short Cu–N distances, two short Cu–O distances, and one elongated Cu–N distance to the ligand in the apical position (Table 1). Complexes **2**–**4**, as well as **6**,[85] display the imino group in the apical position. The *N*-dipp complex, **5**, coordinates the pyridyl group in the

DOI: 10.1021/acs.organomet.8b00196
Organometallics XXXX, XXX, XXX–XXX

apical position instead of the imine (Figure 1, Table 1). While it is tempting to ascribe this to the increased steric bulk of the diip substituent, coordination of the pyridyl group in the apical position was also favored upon reducing the steric bulk from *N*-CH(Me)Ph in **6** to *N*-CH_2Ph in **7**.[84,85] In general, bond distances and angles do not show any clear dependence on the bulk of the N-imino substituent. In concurrence with earlier findings, iminopyrrolide complexes **2**–**5** thus show an invariant structural motif (square-pyramidal coordination with the anionic ligands in equatorial positions) combined with a flexibility of the remaining coordination geometry.

Lactide Polymerization. Complexes **2**–**5** were tested for the polymerization of *rac*-lactide at room temperature in C_6D_6 solution (Table 2, Figures S1 and S2). Complex **2** was barely active at all and reached less than 10% conversion even after 24 h, while **3** showed moderate activity, 6–8 times slower than less sterically demanding complexes **6** or **7**, reported previously.[84,85] Slight curvatures in the semilogarithmic conversion–time plot (Figure 2) and 83% final conversion for **3** indicate that this

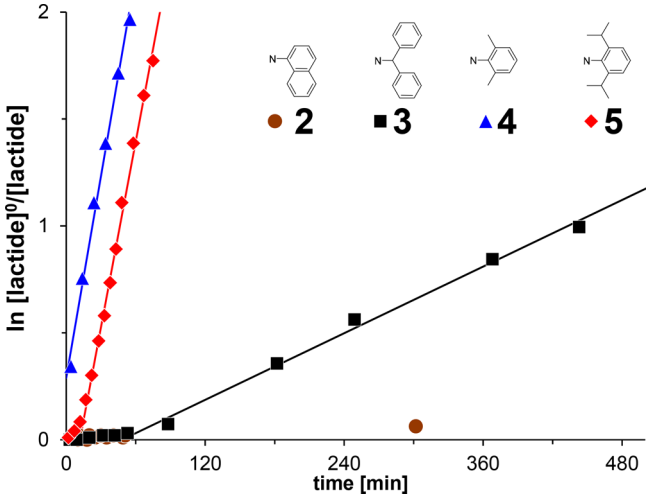

Figure 2. Semilogarithmic conversion–time plot for *rac*-lactide polymerizations with **2** (circles), **3** (squares), **4** (triangles), and **5** (diamonds).

might be partially due to complex decomposition. Complexes **4** and **5**, however, showed even higher activities than those of **6** or **7** (Figure 2, Table 2). Variation of the *ortho*-substituent on the *N*-aryl between methyl and isopropyl did not notably influence activity.

PLA produced with **3** and **5** shows the molecular weight expected for 1 polymer chain per catalysts dimer (Table 2). The lower polymer molecular weight obtained with complex **4** corresponds to 1.7 polymer chains per dimer. The MALDI-MS spectrum of PLA obtained with **4** shows however the presence of cyclic oligomers (Figure S3), which led to the increased number of polymer chains. Stereoerror analysis by ^{13}C NMR of PLA produced with **4** yielded a ratio of *mrm*/*mmr*/*rmm*/*rmr* of 15%:11%:11%:5%, which is the exact ratio expected for chain-end control with a P_m value of 0.69 (Figure 3, Table S1).[112] Monoiminopyrrolide complexes **3**–**5** thus follow the same mechanism as determined for diiminopyrrolide **1** in which only one pyridylmethoxide substituent initiates chain growth and the active species is dinuclear.[85,94]

As generally observed for iminopyrrolide copper complexes, polymer molecular weight control is relatively poor and

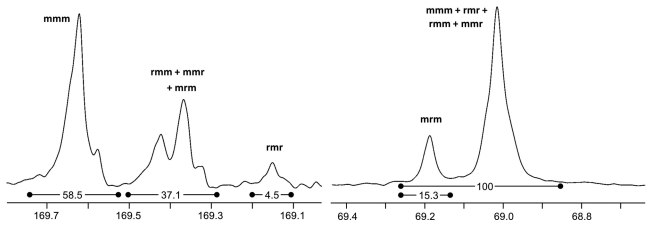

Figure 3. $^{13}C\{^1H\}$-NMR of PLA obtained with **4**. Left: carbonyl region, right: methine region. Tetrad assignments according to refs 113 and 114.

polydispersities of 1.6–1.8 are surprisingly broad for such well-controlled reactions. Broadened polydispersities are most likely associated with the (reversible) formation of an inactive species. Addition of 1 equiv of trityl alcohol has been shown to enforce fast chain-transfer between inactive and active species without generating additional polymer chains.[85] Addition of Ph_3COH to polymerizations with **5** (Figures S4 and S5) consequently reduced polydispersities to 1.3 (Table 2).

Complexes **3**–**5** all produce isotactically enriched PLA. Replacing H or Me in the *N*–CH(R)Ph substituents of **6** and **7** by phenyl did not increase isotacticity and **3** displayed an even lower P_m value (Table 2). *N*-Aryl substituted **4** and **5**, however, showed a notable increase in stereocontrol to P_m = 0.68 and 0.65, respectively. Monoiminopyrrolide complexes thus show a clearer and more pronounced dependence of stereocontrol on ligand bulk than diiminopyrrolide complexes (Scheme 2), which confirms the participation of the ligand environment on monomer selection.

Impact of Site Epimerization on Stereocontrol. In the proposed stereocontrol mechanism, a misinsertion is followed by fast catalytic-site inversion and continued isotactic polymerization (Scheme 3) and would thus produce an isolated *mrm*-tetrad. Contrary to typical chain-end control, the insertion rate, or more precisely the insertion/isomerization rate ratio, can have an influence on stereocontrol. If insertion occurs before isomerization, then an *rmr*-tetrad might be produced, either because the ligand environment is solely responsible for monomer selection or because the chain-end/catalytic-site mismatch decreases stereocontrol. In other words, if epimerization is slow relative to insertion, then the catalyst partially behaves as being either under catalytic-site control or under no stereocontrol, both of which provide lower total isotacticities than pure chain-end control (given the same selectivity, catalytic-site control provides up to 10% less isotactic tetrads than chain-end control in lactide polymerization).

Since insertion rate is dependent on monomer concentration, while epimerization is not, one would thus expect that stereocontrol increases with conversion since lower lactide concentrations favor epimerization. Isotacticities indeed increase during the polymerization in lactide polymerization with **1**,[85] as well as in polymerizations with **3**–**5** (Figures S2 and S5), but the small amount of the changes make it impossible to delineate this effect from chain-end effects at lower chain-lengths. We thus conducted polymerizations with **5** at constant catalyst concentration but varying monomer concentrations (Table S2, Figure S4). Complex **5** was chosen since it was most likely to show slow epimerization and one equiv of Ph_3COH was added to avoid any influence of reversible or irreversible catalyst decomposition on stereocontrol. At higher lactide concentrations which favor insertion over epimerization, stereocontrol was indeed reduced for 0.67 to 0.63 (Table 3,

DOI: 10.1021/acs.organomet.8b00196
Organometallics XXXX, XXX, XXX–XXX

Table 3. *rac*-Lactide Polymerization with 4 at Different Lactide Concentrations[a]

[4]	[lactide]	k_{obs} [h^{-1}]	conversion	P_m[b]
2.0 mM	0.10 M	1.13(2)	98%	0.67
2.0 mM	0.20 M	1.79(3)	95%	0.65
2.0 mM[c]	0.20 M	1.74(8)	99%	0.65
2.0 mM	0.40 M	1.34(5)	97%	0.63

[a]Conditions: C_6D_6, in the presence of 2 mM Ph_3COH. [b]P_m value averaged for a polymerization degree >40 lactide units. Typically at polymerization degrees above 40 units the influence of the chain-end became negligible and P_m values remained constant to ±1% (cf. Figure S5). [c]No Ph_3COH added.

Figure S5). The observed trend thus supports the necessary involvement of catalytic-site epimerization in the mechanism, although the differences were barely larger than the typical error (±2% for P_m in repeated experiments).

On the basis of the provided mechanism, polymerization of enantiopure lactide should be faster than that of *rac*-lactide, since all catalyst would be present in the same isomer enabling isotactic insertion with the full monomer concentration. In *rac*-lactide polymerization, the catalyst is present 50% in *SS*-selective form and 50% in *RR*-selective form, and half of the monomer can only be incorporated by misinsertion (which is by necessity slower). Polymerizations of **5** with *L*-lactide instead of *rac*-lactide showed very similar kinetics with identical induction periods of 11 and 12 min, respectively. As expected, the apparent rate constant for *L*-lactide polymerization was 50% higher (2.85(3) h^{-1} for *L*-lactide compared to that for *rac*-lactide, 1.74(8) h^{-1}). This is a somewhat larger difference than expected and translates to an isotacticity of P_m = 0.82 (see the Supporting Information). While there are possible mechanistic explanations for this, to differentiate between P_m = 0.82 and the observed P_m = 0.66, rate constants would have to be accurate within ±10%. The difference is thus most likely due to the experimental error in working with two different batches of lactide.

Impact of Catalytic-Site Symmetry on Stereocontrol. The proposed stereocontrol mechanism relies on the catalytic site to transfer (and amplify) the chiral information on the chain-end. Accordingly, in the presence of a symmetric catalytic site, no stereocontrol is expected. We have previously reported that **8** carrying a *para*-bromobenzyl *N*-substituent unexpectedly coordinated both iminogroups to the copper center which resulted in a C_s-symmetric catalytic site (Scheme 5).[84] The difference in coordination mode was attributed to increased π-stacking interactions in this complex. To distinguish between effects of catalytic site symmetry and effects due to changes in the substitution pattern, such as increased π-stacking interactions, respective monoiminopyrrolide **9** was prepared (Scheme 5). Contrary to its benzyl analogue **7**, the crystal structure of **9** shows coordination of the imine in the apical position (Figure 4), again indicating that the different

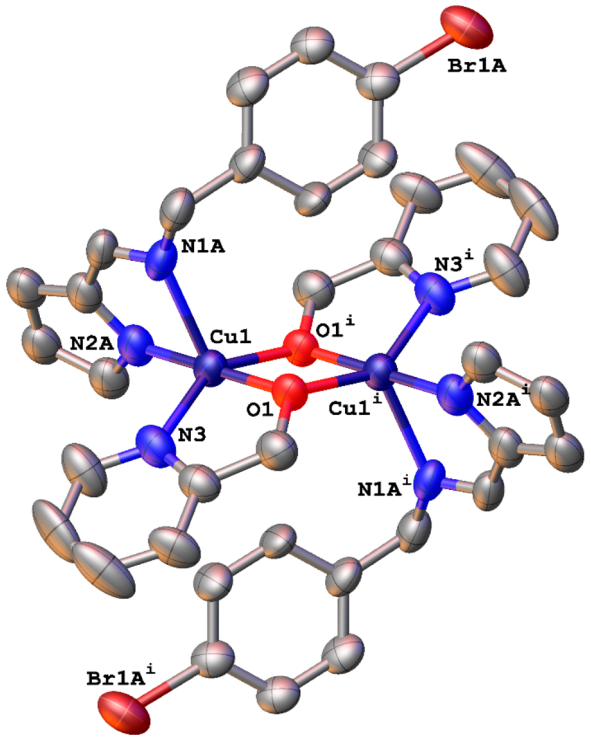

Figure 4. Crystal structure of **9**. Hydrogen atoms and the minor part of the disorder omitted for clarity. Thermal ellipsoids shown at the 50% probability level.

coordination isomers observed in solid state are likely very close in energy. Bond lengths and angles are similar to those of **2**–**4** and **6** (Table 1).

While **9** can provide the same interactions as **8**, it cannot form a C_s-symmetric complex and thus allows us to delineate between the two influences. *rac*-Lactide polymerization with **9** followed clean first-order kinetics (Figures S8 and S9) with a rate constant approximately half of that of the respective benzyl-substituted complex **7**. Polymer molecular weight data corresponded to one pyridylmethoxide per catalyst dimer initiating polymerization but was slightly depressed from that value (Table 2). MALDI-MS analysis again indicated the presence of intramolecular transesterification reactions (Figure S10).

More importantly, monoiminopyrrolide complex **9** showed isotactic stereocontrol identical to that of its *N*-benzyl analogue **7** (P_m = 0.60 in both cases, Table 2), thus indicating a negligible influence of the *para*-bromosubstituent on stereocontrol. In *rac*-lactide polymerizations with **8**, however, atactic PLA (P_m = 0.53) was obtained, with C_s-symmetric **8** being the only pyridylmethoxide containing complex investigated which did *not* produce isotactically enriched PLA.[84,85,94] This strongly supports that the chirality of the catalytic site is responsible for monomer selection, even though stereoerror analysis and other data clearly indicated that the chiral information is provided by the chain-end.

CONCLUSION

Investigations into monoiminopyrrolide complexes showed that their lactide polymerization behavior models that of their

Scheme 5

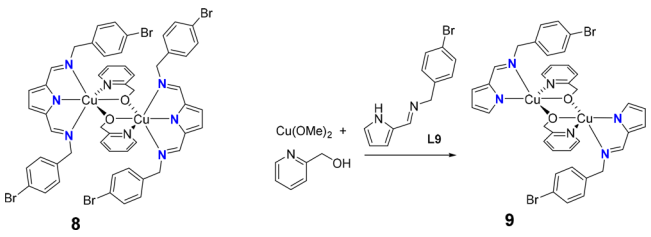

DOI: 10.1021/acs.organomet.8b00196
Organometallics XXXX, XXX, XXX−XXX

respective diiminopyrrolide analogues. The observed impact of ligand congestion on stereocontrol, the dependence of stereocontrol on monomer concentration, and most importantly, the absence of stereocontrol if the catalytic site becomes symmetrical strongly support the presence of a catalytic-site-mediated chain-end control mechanism in this type of complexes.

Despite the advantages inherent with this stereocontrol mechanism, a successful application will have to rely on establishing the same mechanism in a different catalytic system. Although iminopyrrolide complexes provided the only isotactic copper complexes reported so far, their inherent weaknesses (poor molecular weight control, sluggish response to steric bulk, and limited synthetic variability) where again underlined in this study and make it unlikely that this class of complexes can be improved much further.

EXPERIMENTAL SECTION

General Considerations. All reactions were carried out using Schlenk or glovebox techniques under nitrogen atmosphere. $Cu(OMe)_2$,[115] **L4**,[116] and **L5**[117] were prepared according to literature. 1*H*-Pyrrole-2-dicarbaldehyde was prepared according to literature and recrystallized from hexane at −80 °C.[118] Solvents were dried by passage through activated aluminum oxide (MBraun SPS), deoxygenated by repeated extraction with nitrogen, and stored over molecular sieves. C_6D_6 was dried over molecular sieves. *rac*-Lactide (98%) was purchased from Sigma−Aldrich, purified by 3× recrystallization from dry ethyl acetate and kept at −30 °C. All other chemicals were purchased from common commercial suppliers and used without further purification. ^1H and ^{13}C NMR spectra were acquired on Bruker Avance 300 and 400 spectrometers. Chemical shifts were referenced to the residual signals of the deuterated solvents ($CDCl_3$: ^1H: δ 7.26 ppm, ^{13}C: δ 77.16; C_6D_6: ^1H: δ 7.16 ppm, ^{13}C: δ 128.38 ppm). Elemental analyses were performed by the Laboratoire d'analyse élémentaire (Université de Montréal). All UV−vis measurements were conducted in anhydrous and degassed toluene at room temperature in a sealed quartz cell on a Cary 500i UV−vis−NIR spectrophotometer.

2-((Naphthyl)aldimino)pyrrole, L2. 1*H*-Pyrrole-2-carbaldehyde (1.0 g, 11 mmol) was dissolved in dry toluene (25 mL). $MgSO_4$ (5 g), a catalytic amount of Amberlyst 15, and 1-naphtylamine (1.5 g, 11 mmol) were added. The reaction mixture was stirred overnight at room temperature. The brown suspension was filtered, and the solvent was removed under vacuum. The residue was treated with hexane (20 mL), resulting in a brown oil. The oil was separated by decantation and dried under vacuum (1.8 g, 78%). The ^1H NMR spectra is identical to an alternative preparation published earlier.[119]

^1H NMR ($CDCl_3$, 400 MHz,): δ 8.35−8.27 (m, 2H, (N═C)H and Ar), 7.85 (d, J_{HH} = 7 Hz, 1H, Ar), 7.70 (d, J_{HH} = 8 Hz, 1H, Ar), 7.55−7.42 (m, 3H, Ar), 7.27−7.25 (m, 1H, Ar), 7.05 (d, $^3J_{HH}$ = 7 Hz, 1H, 5-pyrrole), 7.03 (br s, 1H, NH), 6.76−6.72 (m, 1H, 3-pyrrole), 6.38−6.31 (m, 1H, 4-pyrrole).

2-((Benzylhydryl)aldimino)pyrrole, L3. Analogous to **L2**, from 1*H*-pyrrole-2-carbaldehyde (1.0 g, 11 mmol) and benzhydrylamine (1.9 g, 11 mmol) to yield a brown oil (2.2 g, 81%). The ^1H NMR spectra is identical to an alternative preparation published earlier.[120]

^1H NMR ($CDCl_3$, 400 MHz,): δ 8.43 (br s, 1H, NH), 7.97 (s, 1H, (N═C)H), 7.33−7.16 (m, 10H, Ph), 6.98−6.93 (m, 1H, 5-pyrrole), 6.56 (d, $^3J_{HH}$ = 4 Hz, 1H, 3-pyrrole), 6.21 (dd, $^3J_{HH}$ = 4, 3 Hz, 1H, 4-pyrrole), 5.62 (s, 1H, CH).

2-((4-Bromobenzyl)aldimino)pyrrole, L9. Analogous to **L2**, from 1*H*-pyrrole-2-carbaldehyde (1.0 g, 11 mmol) and *p*-bromobenzylamine (2.9 g, 16 mmol) to give 2.5 g (91%) of a 1:3 mixture of *p*-bromobenzylamine and **L9**. Purification attempts were unsuccessful and the mixture was used without purification in further synthesis.

^1H NMR ($CDCl_3$, 300 MHz): δ 8.15 (dd, J_{HH} = 2, 1 Hz, 1H, ((N═)C)H), 7.49−7.41 (m, 2H, Ar), 7.19−7.14 (m, 2H, Ar), 6.90−6.86 (m, 1H, 5-pyrrole), 6.53 (dd, $^3J_{HH}$ = 4, $^4J_{HH}$ = 1 Hz, 1H, 3-pyrrole), 6.25 (dd, $^3J_{HH}$ = 4, 3 Hz, 1H, 4-pyrrole), 4.65 (s, 2H, CH_2). $^{13}C\{^1H\}$ NMR ($CDCl_3$, 75 MHz): δ 152.8 (N═C), 138.8 (*ipso*-Ph), 131.7 (*m*-Ph), 130.0 (2-pyrrole), 129.7 (*o*-Ph), 122.1 (5-pyrrole), 121.0 (*p*-Ph), 114.8 (3-pyrrole), 110.1 (4-pyrrole), 63.8 (CH_2). ESI-HRMS (*m*/*z*): M + H^+ ($C_{12}H_{12}BrN_2$) calcd 263.0178; found: 263.0189.

(L2)$_2$Cu$_2$(μ-O,κ_N-OCH$_2$Py)$_2$, 2. $Cu(OMe)_2$ (57 mg, 0.45 mmol) was suspended in toluene (3 mL). 2-Pyridylmethanol (87 μL, 0.90 mmol) was added to the blue suspension, which was stirred for 45 min. A freshly prepared brown solution of **L2** (100 mg, 0.45 mmol) in toluene (2 mL) was added dropwise, resulting in a dark green solution. The reaction was stirred 48 h at RT, filtered to remove trace impurities, concentrated to 1/3 of the volume, diluted with hexane (18 mL), and kept at −30 °C for 4 h, resulting in 31 mg (18%) of green X-ray-quality crystals. Samples for elemental analysis were obtained by diffusion of hexane into dichloromethane (1:3).

UV−vis (toluene, 2.3 × 10^{-6} M) λ_{max}, nm (ε, mol^{-1} cm^2): 355 (25 200), 522 (sh), 603 (252), 666 (200). Anal. Calcd for $C_{42}H_{34}Cu_2N_6O_2$: C, 64.52; H, 4.38; N, 10.75; Found: C, 65.09; H, 4.99; N, 11.33. (Recrystallized twice, final result shown.)

(L3)$_2$Cu$_2$(μ-O,κ_N-OCH$_2$Py)$_2$, 3. Analogous to **2**, from $Cu(OMe)_2$ (48 mg, 0.38 mmol) in toluene (3 mL), 2-pyridylmethanol (73 μL, 0.76 mmol), and **L3** (100 mg, 0.38 mmol) in toluene (2 mL) afforded 32 mg (20%) of green X-ray-quality crystals. Samples for elemental analysis were obtained by diffusion of hexane into dichloromethane (1:3).

UV−vis (toluene, 2 × 10^{-6} M) λ_{max}, nm (ε, mol^{-1} cm^2): 364 (4700), 509 (550), 603 (500), 671 (470). Anal. Calcd for $C_{48}H_{42}Cu_2N_6O_2 \cdot 1/4CH_2Cl_2$: C, 65.62; H, 4.85; N, 9.52; Found: C, 66.03; H, 4.96; N, 9.90.

(L4)$_2$Cu$_2$(μ-O,κ_N-OCH$_2$Py)$_2$, 4. Analogous to **2**, from $Cu(OMe)_2$ (63 mg, 0.50 mmol) in toluene (3 mL), 2-pyridylmethanol (96 μL, 1.0 mmol), and **L4** (100 mg, 0.50 mmol) in toluene (2 mL) afforded 41 mg (23%) of green X-ray-quality crystals. Samples for elemental analysis were obtained by diffusion of hexane into dichloromethane (1:3).

UV−vis (toluene, 2.5 × 10^{-6} M) λ_{max}, nm (ε, mol^{-1} cm^2): 350 (21 400), 388 (sh), 542 (780), 607 (800), 664 (675). Anal. Calcd for $C_{38}H_{38}Cu_2N_6O_2 \cdot 1/4CH_2Cl_2$: C, 60.52; H, 5.11; N, 11.07; Found: C, 60.72; H, 5.15; N, 11.36.

(L5)$_2$Cu$_2$(μ-O,κ_N-OCH$_2$Py)$_2$, 5. Analogous to **2**, from $Cu(OMe)_2$ (49 mg, 0.39 mmol) in toluene (3 mL), 2-pyridylmethanol (75 μL, 0.78 mmol), and **L5** (100 mg, 0.39 mmol) in toluene (2 mL) afforded 40 mg (24%) of green X-ray-quality crystals. Samples for elemental analysis were obtained by diffusion of hexane into dichloromethane (1:3).

UV−vis (toluene, 3.6 × 10^{-5} M) λ_{max}, nm (ε, mol^{-1} cm^2): 355 (18 500), 388 (sh), 472 (1400), 673 (320). Anal. Calcd for $C_{46}H_{54}Cu_2N_6O_2$: C, 65.00; H, 6.40; N, 9.89; Found: C, 64.60; H, 6.10; N, 9.78.

(L9)$_2$Cu$_2$(μ-O,κ_N-OCH$_2$Py)$_2$, 9. Analogous to **2**, from $Cu(OMe)_2$ (50 mg, 0.40 mmol) in toluene (3 mL), 2-pyridylmethanol (77 μL, 0.80 mmol), and **L9** (100 mg, 0.40 mmol) in toluene (2 mL). Decantation and washing with hexane (3 × 10 mL) afforded 31 mg (18%) of green X-ray quality crystals.

UV−vis (toluene, 1.2 × 10^{-5} M) [λ_{max}, nm (ε, mol^{-1} cm^2)]: 351 (18 600), 371 (sh), 490 (1200), 603 (800), 664 (720). Anal. Calcd for $C_{36}H_{32}Br_2Cu_2N_6O_2$: C, 49.84; H, 3.72; N, 9.69; Found: C, 50.06; H, 3.73; N, 9.43.

***rac*-Lactide Polymerization.** All manipulations took place in a glovebox under nitrogen atmosphere. Stock solutions of the catalysts and BnOH were prepared in dry C_6D_6 and stored at −30 °C to avoid concentration changes. The desired amount of *rac*-lactide was placed into a J. Young tube together with C_6D_6. A stock solution of benzyl alcohol was added, where required, followed by a stock solution of the catalyst (ca. 20 mM in C_6D_6) to give final concentrations of 2.0 mM catalyst dimer and of 0.20 M lactide. After complete dissolution was assured by shaking, the reaction was followed by ^1H NMR. The reaction was quenched by addition of 5−10 equiv of a $CDCl_3$ solution

DOI: 10.1021/acs.organomet.8b00196
Organometallics XXXX, XXX, XXX−XXX

Table 4. Details of X-ray Diffraction Experiments

	2	3	4	5	9
formula	$C_{42}H_{34}Cu_2N_6O_2$	$C_{48}H_{42}Cu_2N_6O_2$	$C_{38}H_{38}Cu_2N_6O_2$	$C_{46}H_{54}Cu_2N_6O_2$	$C_{36}H_{32}Br_2Cu_2N_6O_2$
M_w (g/mol); d_{calcd} (g/cm^3)	781.83; 1.201	861.95; 1.428	737.82; 1.410	850.03; 1.303	867.57; 1.696
T (K); $F(000)$	150; 3618	150; 892	150; 764	150; 446	150; 868
crystal system	trigonal	monoclinic	triclinic	triclinic	monoclinic
space group	$R\bar{3}$	$P2_1/c$	$P\bar{1}$	$P\bar{1}$	$P2_1/c$
unit cell					
a (Å)	35.261(5)	8.8407(3)	7.9918(7)	10.2561(6)	11.7994(7)
b (Å)	35.261(5)	16.3755(5)	12.0774(12)	10.8248(6)	20.5590(13)
c (Å)	9.0334(17)	14.1657(4)	18.2565(17)	11.7883(7)	7.0097(4)
α (deg)	90	90	95.832(5)	65.984(3)	90
β (deg)	90	102.2090(10)	95.745(5)	83.830(3)	92.497(4)
γ (deg)	120	90	94.455(5)	65.374(3)	90
V (Å^3); Z	9727(3); 9	2004.40(11); 2	1737.3(3); 2	1083.67(11); 1	1698.83(18); 2
μ (mm^{-1}); abs. corr.	5.51; multiscan	5.98; multiscan	6.83; multiscan	5.52; multiscan	8.90; multiscan
θ range (deg); completeness	2.2−33.6; 0.99	3.6−60.7; 0.98	3.2−61.3; 0.96	3.6−59.9; 0.99	3.3−55.9; 0.99
collected reflections; R_σ	9578; 0.183	28616; 0.026	67959; 0.126	27019; 0.052	34561; 0.059
unique reflections; R_{int}	1320; 0.251	4539; 0.046	7954; 0.186	4963; 0.079	3889; 0.099
$R_1(F)$ ($I > 2\sigma(I)$)	0.114	0.039	0.126	0.082	0.103
$wR(F^2)$ (all data)	0.299	0.107	0.351	0.233	0.259
GoF (F^2)	1.07	1.11	1.08	1.06	1.08
residual electron density	0.48, −0.28	0.32, −0.95	1.07, −0.82	1.41, −0.77	1.04, −0.69

of acetic acid (10 mM, drops). The volatiles were evaporated and solid polymer samples were stored at −80 °C for further analysis.

Conversion was determined from ^{1}H NMR by comparison to remaining lactide. P_m values were determined from homodecoupled ^{1}H NMR spectra and calculated from $P_m = 1 - 2{\cdot}I_1/(I_1 + I_2)$, with I_1 = 5.15−5.21 ppm (*rmr*, *mmr*/*rmm*), I_2 = 5.21−5.25 ppm (*mmr*/*rmm*, *mmm*, *mrm*). The integration of the left multiplet and right multiplet (I_1 and I_2) required only one very reproducible dividing point of the integration, which was always taken as the minimum between the two multiplets. P_m values obtained this way were typically consistent to ±1% over the course of one experiment and ±3% between different experiments under identical conditions. Molecular weight analyses were performed on a Waters 1525 gel permeation chromatograph equipped with three Phenomenex columns and a refractive index detector at 35 °C. THF was used as the eluent at a flow rate of 1.0 mL·min^{-1} and polystyrene standards (Sigma−Aldrich, 1.5 mg·mL^{-1}, prepared and filtered (0.2 mm) directly prior to injection) were used for calibration. Obtained molecular weights were corrected by a Mark−Houwink factor of 0.58.[121]

X-ray Diffraction. Single crystals were obtained directly from isolation of the products as described above. Diffraction data were collected on a Bruker Venture METALJET diffractometer (Ga Kα radiation) using the APEX2 software package.[122] Data reduction was performed with SAINT,[123] and absorption corrections were carried out with SADABS.[124] Structures were solved by dual-space methods (SHELXT).[125] All non-hydrogen atoms were refined anisotropic using full-matrix least-squares on F^2 and hydrogen atoms refined with fixed isotropic U using a riding model (SHELXL2014).[126] Complexes **2**, **4**, and **9** were found to be twinned. Complex **2** diffracted very weakly, and a general thermal parameter restraint (RIGU) was necessary in refinement due to the resulting bad data quality. No better crystal could be obtained. Further experimental details can be found in Table 4 and in the Supporting Information.

■ ASSOCIATED CONTENT

Supporting Information

The Supporting Information is available free of charge on the ACS Publications website at DOI: 10.1021/acs.organomet.8b00196.

Additional tables and figures (PDF)

Accession Codes

CCDC 1581210−1581214 contain the supplementary crystallographic data for this paper. These data can be obtained free of charge via www.ccdc.cam.ac.uk/data_request/cif, or by emailing data_request@ccdc.cam.ac.uk, or by contacting The Cambridge Crystallographic Data Centre, 12 Union Road, Cambridge CB2 1EZ, UK; fax: +44 1223 336033.

■ AUTHOR INFORMATION

Corresponding Author

*E-mail: Frank.Schaper@umontreal.ca.

ORCID

Frank Schaper: 0000-0002-3621-8920

Notes

The authors declare no competing financial interest.

■ ACKNOWLEDGMENTS

Funding was supplied by the NSERC discovery program (RGPIN-2016-04953) and the Centre for Green Chemistry and Catalysis (FQRNT). We thank Francine Bélanger for support with X-ray diffraction, Elena Nadezhina for elemental analysis, and Marie-Christine Tang, Karine Gilbert and Dr. Alexandra Furtos for support with MALDI-MS. Polymerization with *L*-lactide was proposed by a reviewer.

■ REFERENCES

(1) Nagarajan, V.; Mohanty, A. K.; Misra, M. *ACS Sustainable Chem. Eng.* **2016**, *4*, 2899−2916.

(2) Castro-Aguirre, E.; Iñiguez-Franco, F.; Samsudin, H.; Fang, X.; Auras, R. *Adv. Drug Delivery Rev.* **2016**, *107*, 333−366.

(3) Slomkowski, S.; Penczek, S.; Duda, A. *Polym. Adv. Technol.* **2014**, *25*, 436−447.

(4) Singhvi, M.; Gokhale, D. *RSC Adv.* **2013**, *3*, 13558−13568.

(5) Hottle, T. A.; Bilec, M. M.; Landis, A. E. *Polym. Degrad. Stab.* **2013**, *98*, 1898−1907.

(6) Inkinen, S.; Hakkarainen, M.; Albertsson, A.-C.; Södergård, A. *Biomacromolecules* **2011**, *12*, 523−532.

(7) Ahmed, J.; Varshney, S. K. *Int. J. Food Prop.* **2011**, *14*, 37−58.

DOI: 10.1021/acs.organomet.8b00196
Organometallics XXXX, XXX, XXX−XXX

(8) Vijayakumar, J.; Aravindan, R.; Viruthagiri, T. *Chem. Biochem. Eng. Q.* **2008**, *22*, 245−264.
(9) Tokiwa, Y.; Calabia, B. P. *Can. J. Chem.* **2008**, *86*, 548−555.
(10) Drumright, R. E.; Gruber, P. R.; Henton, D. E. *Adv. Mater. (Weinheim, Ger.)* **2000**, *12*, 1841−1846.
(11) Vink, E. T. H.; Rábago, K. R.; Glassner, D. A.; Springs, B.; O'Connor, R. P.; Kolstad, J.; Gruber, P. R. *Macromol. Biosci.* **2004**, *4*, 551−564.
(12) Paul, S.; Zhu, Y.; Romain, C.; Brooks, R.; Saini, P. K.; Williams, C. K. *Chem. Commun. (Cambridge, U. K.)* **2015**, *51*, 6459−6479.
(13) dos Santos Vieira, I.; Herres-Pawlis, S. *Eur. J. Inorg. Chem.* **2012**, *2012*, 765−774.
(14) Dutta, S.; Hung, W.-C.; Huang, B.-H.; Lin, C.-C. Recent Developments in Metal-Catalyzed Ring-Opening Polymerization of Lactides and Glycolides: Preparation of Polylactides, Polyglycolide, and Poly(lactide-co-glycolide). In *Synthetic Biodegradable Polymers*; Rieger, B., Künkel, A., Coates, G. W., Reichardt, R., Dinjus, E., Zevaco, T. A., Eds.; Springer-Verlag: Berlin, 2011; pp 219−284.
(15) Dijkstra, P. J.; Du, H.; Feijen, J. *Polym. Chem.* **2011**, *2*, 520−527.
(16) Buffet, J.-C.; Okuda, J. *Polym. Chem.* **2011**, *2*, 2758−2763.
(17) Thomas, C. M. *Chem. Soc. Rev.* **2010**, *39*, 165.
(18) Stanford, M. J.; Dove, A. P. *Chem. Soc. Rev.* **2010**, *39*, 486−494.
(19) Williams, C. K.; Hillmyer, M. A. *Polym. Rev.* **2008**, *48*, 1−10.
(20) Ajellal, N.; Carpentier, J.-F.; Guillaume, C.; Guillaume, S. M.; Helou, M.; Poirier, V.; Sarazin, Y.; Trifonov, A. *Dalton Trans.* **2010**, *39*, 8363.
(21) Platel, R. H.; Hodgson, L. M.; Williams, C. K. *Polym. Rev.* **2008**, *48*, 11−63.
(22) Wu, J.; Yu, T.-L.; Chen, C.-T.; Lin, C.-C. *Coord. Chem. Rev.* **2006**, *250*, 602−626.
(23) Dechy-Cabaret, O.; Martin-Vaca, B.; Bourissou, D. *Chem. Rev.* **2004**, *104*, 6147−6176.
(24) O'Keefe, B. J.; Hillmyer, M. A.; Tolman, W. B. *J. Chem. Soc., Dalton Trans.* **2001**, 2215−2224.
(25) Chisholm, M. H.; Zhou, Z. *J. Mater. Chem.* **2004**, *14*, 3081.
(26) Zhong, Z.; Dijkstra, P. J.; Feijen, J. *J. Biomater. Sci., Polym. Ed.* **2004**, *15*, 929−946.
(27) Huang, B. H.; Dutta, S.; Lin, C. C. 1.39-Main-Group Catalysts for Lactide Polymerization. In *Comprehensive Inorganic Chemistry II*, 2nd ed.; Poeppelmeier, J. R., Ed.; Elsevier: Amsterdam, 2013; pp 1217−1249.
(28) Wheaton, C. A.; Hayes, P. G. *Comments Inorg. Chem.* **2011**, *32*, 127−162.
(29) Wheaton, C. A.; Hayes, P. G.; Ireland, B. J. *Dalton Trans.* **2009**, 4832−4846.
(30) Sutar, A. K.; Maharana, T.; Dutta, S.; Chen, C.-T.; Lin, C.-C. *Chem. Soc. Rev.* **2010**, *39*, 1724−1746.
(31) Le Roux, E. *Coord. Chem. Rev.* **2016**, *306*, 65−85.
(32) Sauer, A.; Kapelski, A.; Fliedel, C.; Dagorne, S.; Kol, M.; Okuda, J. *Dalton Trans.* **2013**, *42*, 9007−9023.
(33) MacDonald, J. P.; Shaver, M. P. Aluminum Salen and Salan Polymerization Catalysts: From Monomer Scope to Macrostructure Control. In *Green Polymer Chemistry: Biobased Materials and Biocatalysis*; American Chemical Society: Washington, DC, 2015; Vol. *1192*, pp 147−167.
(34) Jianming, R.; Anguo, X.; Hongwei, W.; Hailin, Y. *Des. Monomers Polym.* **2014**, *17*, 345−355.
(35) Dagorne, S.; Normand, M.; Kirillov, E.; Carpentier, J.-F. *Coord. Chem. Rev.* **2013**, *257*, 1869−1886.
(36) Dagorne, S.; Fliedel, C. Organoaluminum Species in Homogeneous Polymerization Catalysis. In *Modern Organoaluminum Reagents: Preparation, Structure, Reactivity and Use*; Woodward, S., Dagorne, S., Eds. Springer Berlin Heidelberg: Berlin, Heidelberg, 2013; pp 125−171.
(37) Dagorne, S.; Fliedel, C.; de Frémont, P. Gallium and Indium Compounds in Homogeneous Catalysis. In *Encyclopedia of Inorganic and Bioinorganic Chemistry*; John Wiley & Sons, Ltd: Chichester, West Sussex, U.K., 2011.
(38) Amgoune, A.; Thomas, C. M.; Carpentier, J.-F. *Pure Appl. Chem.* **2007**, *79*, 2013−2030.
(39) Xu, T.-Q.; Yang, G.-W.; Liu, C.; Lu, X.-B. *Macromolecules* **2017**, *50*, 515−522.
(40) Bhattacharjee, J.; Harinath, A.; Nayek, H. P.; Sarkar, A.; Panda, T. K. *Chem. - Eur. J.* **2017**, *23*, 9319−9331.
(41) Myers, D.; White, A. J. P.; Forsyth, C. M.; Bown, M.; Williams, C. K. *Angew. Chem., Int. Ed.* **2017**, *56*, 5277−5282.
(42) Rosen, T.; Popowski, Y.; Goldberg, I.; Kol, M. *Chem. - Eur. J.* **2016**, *22*, 11533−11536.
(43) Sun, Y.; Xiong, J.; Dai, Z.; Pan, X.; Tang, N.; Wu, J. *Inorg. Chem.* **2016**, *55*, 136−143.
(44) McKeown, P.; Davidson, M. G.; Kociok-Kohn, G.; Jones, M. D. *Chem. Commun. (Cambridge, U. K.)* **2016**, *52*, 10431−10434.
(45) Wang, H.; Yang, Y.; Ma, H. *Macromolecules* **2014**, *47*, 7750−7764.
(46) Mou, Z.; Liu, B.; Wang, M.; Xie, H.; Li, P.; Li, L.; Li, S.; Cui, D. *Chem. Commun. (Cambridge, U. K.)* **2014**, *50*, 11411−11414.
(47) Bakewell, C.; White, A. J. P.; Long, N. J.; Williams, C. K. *Angew. Chem., Int. Ed.* **2014**, *53*, 9226−9230.
(48) Aluthge, D. C.; Patrick, B. O.; Mehrkhodavandi, P. *Chem. Commun. (Cambridge, U. K.)* **2013**, *49*, 4295−4297.
(49) Balasanthiran, V.; Chatterjee, C.; Chisholm, M. H.; Harrold, N. D.; RajanBabu, T. V.; Warren, G. A. *J. Am. Chem. Soc.* **2015**, *137*, 1786−1789.
(50) Daneshmand, P.; Schaper, F. *Dalton Trans.* **2015**, *44*, 20449−20458.
(51) Rajashekhar, B.; Chakraborty, D. *Polym. Bull.* **2014**, *71*, 2185−2203.
(52) Idage, B. B.; Idage, S. B.; Kasegaonkar, A. S.; Jadhav, R. V. *Mater. Sci. Eng., B* **2010**, *168*, 193−198.
(53) Kricheldorf, H. R.; Damrau, D.-O. *J. Macromol. Sci., Part A: Pure Appl.Chem.* **1998**, *35*, 1875−1887.
(54) Tschan, M. J. L.; Guo, J.; Raman, S. K.; Brule, E.; Roisnel, T.; Rager, M.-N.; Legay, R.; Durieux, G.; Rigaud, B.; Thomas, C. M. *Dalton Trans.* **2014**, *43*, 4550−4564.
(55) Shin, S.; Nayab, S.; Lee, H. *Polyhedron* **2018**, *141*, 309−321.
(56) Duan, R.; Hu, C.; Li, X.; Pang, X.; Sun, Z.; Chen, X.; Wang, X. *Macromolecules* **2017**, *50*, 9188−9195.
(57) Delle Chiaie, K. R.; Biernesser, A. B.; Ortuno, M. A.; Dereli, B.; Iovan, D. A.; Wilding, M. J. T.; Li, B.; Cramer, C. J.; Byers, J. A. *Dalton Trans.* **2017**, *46*, 12971−12980.
(58) Herber, U.; Hegner, K.; Wolters, D.; Siris, R.; Wrobel, K.; Hoffmann, A.; Lochenie, C.; Weber, B.; Kuckling, D.; Herres-Pawlis, S. *Eur. J. Inorg. Chem.* **2017**, *2017*, 1341−1354.
(59) Brown, L. A.; Wekesa, F. S.; Unruh, D. K.; Findlater, M.; Long, B. K. *J. Polym. Sci., Part A: Polym. Chem.* **2017**, *55*, 2824−2830.
(60) Delle Chiaie, K. R.; Yablon, L. M.; Biernesser, A. B.; Michalowski, G. R.; Sudyn, A. W.; Byers, J. A. *Polym. Chem.* **2016**, *7*, 4675−4681.
(61) Biernesser, A. B.; Delle Chiaie, K. R.; Curley, J. B.; Byers, J. A. *Angew. Chem., Int. Ed.* **2016**, *55*, 5251−5254.
(62) Silvino, A. C.; Rodrigues, A. L. C.; Resende, J. A. L. C. *Inorg. Chem. Commun.* **2015**, *55*, 39−42.
(63) Manna, C. M.; Kaur, A.; Yablon, L. M.; Haeffner, F.; Li, B.; Byers, J. A. *J. Am. Chem. Soc.* **2015**, *137*, 14232−14235.
(64) Kundys, A.; Plichta, A.; Florjańczyk, Z.; Frydrych, A.; Żurawski, K. *J. Polym. Sci., Part A: Polym. Chem.* **2015**, *53*, 1444−1456.
(65) Keuchguerian, A.; Mougang-Soume, B.; Schaper, F.; Zargarian, D. *Can. J. Chem.* **2015**, *93*, 594−601.
(66) Kang, Y. Y.; Park, H.-R.; Lee, M. H.; An, J.; Kim, Y.; Lee, J. *Polyhedron* **2015**, *95*, 24−29.
(67) Giese, S. O. K.; Egevardt, C.; Rüdiger, A. L.; Sá, E. L.; Silva, T. A.; Zawadzki, S. F.; Soares, J. F.; Nunes, G. G. *J. Braz. Chem. Soc.* **2015**, *26*, 2258−2268.
(68) Manna, C. M.; Kaplan, H. Z.; Li, B.; Byers, J. A. *Polyhedron* **2014**, *84*, 160−167.
(69) Lei, Y.-N.; Zhu, Y.-B.; Gong, C.-F.; Lv, J.-J.; Kang, C.; Hou, L.-X. *J. Mater. Sci.: Mater. Med.* **2014**, *25*, 273−282.

DOI: 10.1021/acs.organomet.8b00196
Organometallics XXXX, XXX, XXX−XXX

(70) Egevardt, C.; Giese, S. O. K.; da C. Santos, A. D.; Barison, A.; de Sá, E. L.; Filho, A. Z.; da Silva, T. A.; Zawadzki, S. F.; Soares, J. F.; Nunes, G. G. *J. Polym. Sci., Part A: Polym. Chem.* **2014**, *52*, 2509−2517.
(71) Biernesser, A. B.; Li, B.; Byers, J. A. *J. Am. Chem. Soc.* **2013**, *135*, 16553−16560.
(72) Chen, J.; Gorczynski, J. L.; Zhang, G.; Fraser, C. L. *Macromolecules* **2010**, *43*, 4909−4920.
(73) Wang, X.; Liao, K.; Quan, D.; Wu, Q. *Macromolecules* **2005**, *38*, 4611−4617.
(74) Gorczynski, J. L.; Chen, J.; Fraser, C. L. *J. Am. Chem. Soc.* **2005**, *127*, 14956−14957.
(75) McGuinness, D. S.; Marshall, E. L.; Gibson, V. C.; Steed, J. W. *J. Polym. Sci., Part A: Polym. Chem.* **2003**, *41*, 3798−3803.
(76) O'Keefe, B. J.; Breyfogle, L. E.; Hillmyer, M. A.; Tolman, W. B. *J. Am. Chem. Soc.* **2002**, *124*, 4384−4393.
(77) Gibson, V. C.; Marshall, E. L.; Navarro-Llobet, D.; White, A. J. P.; Williams, D. J. *J. Chem. Soc., Dalton Trans.* **2002**, 4321−4322.
(78) O'Keefe, B. J.; Monnier, S. M.; Hillmyer, M. A.; Tolman, W. B. *J. Am. Chem. Soc.* **2001**, *123*, 339−340.
(79) Stolt, M.; SödergÅrd, A. *Macromolecules* **1999**, *32*, 6412−6417.
(80) SödergÅrd, A.; Stolt, M. *Macromol. Symp.* **1998**, *130*, 393−402.
(81) Kricheldorf, H. R.; Damrau, D.-O. *Macromol. Chem. Phys.* **1997**, *198*, 1767−1774.
(82) Kwon, K. S.; Nayab, S.; Jeong, J. H. *Polyhedron* **2017**, *130*, 23−29.
(83) Chun, M. K.; Cho, J.; Nayab, S.; Jeong, J. H. *Bull. Korean Chem. Soc.* **2017**, *38*, 1527−1530.
(84) Daneshmand, P.; Fortun, S.; Schaper, F. *Organometallics* **2017**, *36*, 3860−3877.
(85) Daneshmand, P.; van der Est, A.; Schaper, F. *ACS Catal.* **2017**, *7*, 6289−6301.
(86) Ahn, S. H.; Chun, M. K.; Kim, E.; Jeong, J. H.; Nayab, S.; Lee, H. *Polyhedron* **2017**, *127*, 51−58.
(87) Routaray, A.; Nath, N.; Maharana, T.; Sahoo, P. K.; Das, J. P.; Sutar, A. K. *J. Chem. Sci.* **2016**, *128*, 883−891.
(88) Mandal, M.; Oppelt, K.; List, M.; Teasdale, I.; Chakraborty, D.; Monkowius, U. *Monatsh. Chem.* **2016**, *147*, 1883−1892.
(89) Cho, J.; Nayab, S.; Jeong, J. H. *Polyhedron* **2016**, *113*, 81−87.
(90) Akpan, E. D.; Ojwach, S. O.; Omondi, B.; Nyamori, V. O. *New J. Chem.* **2016**, *40*, 3499−3510.
(91) Routaray, A.; Nath, N.; Mantri, S.; Maharana, T.; Sutar, A. K. *Chin. J. Catal.* **2015**, *36*, 764−770.
(92) Routaray, A.; Nath, N.; Maharana, T.; Sutar, A. *J. Macromol. Sci., Part A: Pure Appl.Chem.* **2015**, *52*, 444−453.
(93) Kwon, K. S.; Cho, J.; Nayab, S.; Jeong, J. H. *Inorg. Chem. Commun.* **2015**, *55*, 36−38.
(94) Fortun, S.; Daneshmand, P.; Schaper, F. *Angew. Chem., Int. Ed.* **2015**, *54*, 13669−13672.
(95) Whitehorne, T. J. J.; Schaper, F. *Can. J. Chem.* **2014**, *92*, 206−214.
(96) Appavoo, D.; Omondi, B.; Guzei, I. A.; van Wyk, J. L.; Zinyemba, O.; Darkwa, J. *Polyhedron* **2014**, *69*, 55−60.
(97) Whitehorne, T. J. J.; Schaper, F. *Inorg. Chem.* **2013**, *52*, 13612−13622.
(98) Li, C.-Y.; Hsu, S.-J.; Lin, C.-l.; Tsai, C.-Y.; Wang, J.-H.; Ko, B.-T.; Lin, C.-H.; Huang, H.-Y. *J. Polym. Sci., Part A: Polym. Chem.* **2013**, *51*, 3840−3849.
(99) Whitehorne, T. J. J.; Schaper, F. *Chem. Commun. (Cambridge, U. K.)* **2012**, *48*, 10334−10336.
(100) Gowda, R. R.; Chakraborty, D. *J. Mol. Catal. A: Chem.* **2011**, *349*, 86−93.
(101) Chen, L.-L.; Ding, L.-Q.; Zeng, C.; Long, Y.; Lü, X.-Q.; Song, J.-R.; Fan, D.-D.; Jin, W.-J. *Appl. Organomet. Chem.* **2011**, *25*, 310−316.
(102) Bhunora, S.; Mugo, J.; Bhaw-Luximon, A.; Mapolie, S.; Van Wyk, J.; Darkwa, J.; Nordlander, E. *Appl. Organomet. Chem.* **2011**, *25*, 133−145.
(103) John, A.; Katiyar, V.; Pang, K.; Shaikh, M. M.; Nanavati, H.; Ghosh, P. *Polyhedron* **2007**, *26*, 4033−4044.
(104) Sun, J.; Shi, W.; Chen, D.; Liang, C. *J. Appl. Polym. Sci.* **2002**, *86*, 3312−3315.
(105) Ma, H.; Spaniol, T. P.; Okuda, J. *Angew. Chem., Int. Ed.* **2006**, *45*, 7818−7821.
(106) Amgoune, A.; Thomas, C. M.; Roisnel, T.; Carpentier, J.-F. *Chem. - Eur. J.* **2006**, *12*, 169−179.
(107) Chmura, A. J.; Chuck, C. J.; Davidson, M. G.; Jones, M. D.; Lunn, M. D.; Bull, S. D.; Mahon, M. F. *Angew. Chem., Int. Ed.* **2007**, *46*, 2280−2283.
(108) Chmura, A. J.; Davidson, M. G.; Frankis, C. J.; Jones, M. D.; Lunn, M. D. *Chem. Commun. (Cambridge, U. K.)* **2008**, 1293−1295.
(109) Jones, M. D.; Hancock, S. L.; McKeown, P.; Schafer, P. M.; Buchard, A.; Thomas, L. H.; Mahon, M. F.; Lowe, J. P. *Chem. Commun. (Cambridge, U. K.)* **2014**, *50*, 15967−15970.
(110) Jones, M. D.; Brady, L.; McKeown, P.; Buchard, A.; Schafer, P. M.; Thomas, L. H.; Mahon, M. F.; Woodman, T. J.; Lowe, J. P. *Chem. Sci.* **2015**, *6*, 5034−5039.
(111) Addison, A. W.; Rao, T. N.; Reedijk, J.; van Rijn, J.; Verschoor, G. C. *J. Chem. Soc., Dalton Trans.* **1984**, 1349−1356.
(112) Chamberlain, B. M.; Cheng, M.; Moore, D. R.; Ovitt, T. M.; Lobkovsky, E. B.; Coates, G. W. *J. Am. Chem. Soc.* **2001**, *123*, 3229−3238.
(113) Kasperczyk, J. E. *Polymer* **1999**, *40*, 5455−5458.
(114) Kasperczyk, J. E. *Macromolecules* **1995**, *28*, 3937−3939.
(115) Singh, J. V.; Baranwal, B. P.; Mehrotra, R. C. *Z. Anorg. Allg. Chem.* **1981**, *477*, 235−240.
(116) Yang, Y.; Liu, B.; Lv, K.; Gao, W.; Cui, D.; Chen, X.; Jing, X. *Organometallics* **2007**, *26*, 4575−4584.
(117) Yang, Y.; Cui, D.; Chen, X. *Dalton Trans.* **2010**, *39*, 3959−3967.
(118) Knizhnikov, V. A.; Borisova, N. E.; Yurashevich, N. Y.; Popova, L. A.; Chernyad'ev, A. Y.; Zubreichuk, Z. P.; Reshetova, M. D. *Russ. J. Org. Chem.* **2007**, *43*, 855−860.
(119) Simionescu, C. I.; Grigoras, M.; Cianga, I.; Olaru, N. *Eur. Polym. J.* **1998**, *34*, 891−898.
(120) Wansapura, C. M.; Juyoung, C.; Simpson, J. L.; Szymanski, D.; Eaton, G. R.; Eaton, S. S.; Fox, S. *J. Coord. Chem.* **2003**, *56*, 975−993.
(121) Save, M.; Schappacher, M.; Soum, A. *Macromol. Chem. Phys.* **2002**, *203*, 889−899.
(122) *APEX2*, release 2.1−0; Bruker AXS Inc.: Madison, WI, 2006.
(123) *SAINT*, release 7.34A; Bruker AXS Inc.: Madison, WI, 2006.
(124) Sheldrick, G. M.. *SADABS*; Bruker AXS Inc.: Madison, WI, 2004.
(125) Sheldrick, G. *Acta Crystallogr., Sect. A: Found. Adv.* **2015**, *71*, 3−8.
(126) Sheldrick, G. M. *Acta Crystallogr., Sect. A: Found. Crystallogr.* **2008**, *64*, 112−122.

DOI: 10.1021/acs.organomet.8b00196
Organometallics XXXX, XXX, XXX−XXX